



Singular surfaces and cusps in symmetric planar 3-RPR manipulators

Michel Coste, Philippe Wenger, Damien Chablat

► To cite this version:

Michel Coste, Philippe Wenger, Damien Chablat. Singular surfaces and cusps in symmetric planar 3-RPR manipulators. IEEE/RSJ International Conference on Intelligent Robots and Systems, Sep 2011, San Francisco, United States. pp.1453-1458, 10.1109/IROS.2011.6094724 . hal-00610313

HAL Id: hal-00610313

<https://hal.science/hal-00610313>

Submitted on 21 Jul 2011

HAL is a multi-disciplinary open access archive for the deposit and dissemination of scientific research documents, whether they are published or not. The documents may come from teaching and research institutions in France or abroad, or from public or private research centers.

L'archive ouverte pluridisciplinaire **HAL**, est destinée au dépôt et à la diffusion de documents scientifiques de niveau recherche, publiés ou non, émanant des établissements d'enseignement et de recherche français ou étrangers, des laboratoires publics ou privés.

Singular surfaces and cusps in symmetric planar 3-RPR manipulators

Michel Coste, Philippe Wenger and Damien Chablat

Abstract—We study in this paper a class of 3-RPR manipulators for which the direct kinematic problem (DKP) is split into a cubic problem followed by a quadratic one. These manipulators are geometrically characterized by the fact that the moving triangle is the image of the base triangle by an indirect isometry. We introduce a specific coordinate system adapted to this geometric feature and which is also well adapted to the splitting of the DKP. This allows us to obtain easily precise descriptions of the singularities and of the cusp edges. These latter second order singularities are important for nonsingular assembly mode changing. We show how to sort assembly modes and use this sorting for motion planning in the joint space.

I. INTRODUCTION

Planar parallel manipulators have received a lot of attention [1], [2], [4]–[19] because of their relative simplicity with respect to their spatial counterparts. Moreover, studying the former may help understand the latter. Planar manipulators with three extensible leg rods, referred to as 3-RPR manipulators, have often been studied. Such manipulators may have up to six assembly modes (AM) [2] and their direct kinematics can be written in a polynomial of degree six [3]. It was first pointed out that to move from one assembly mode to another, the manipulator should cross a singularity [2]. However, [4] showed, using numerical experiments, that this statement is not true in general. More precisely, this statement is only true under some special geometric conditions, such as similar base and mobile platforms [5], [6]. Recently, [7] provided a mathematical proof of the decomposition of the workspace into two aspects (singularity-free regions) using geometric properties of the singularity surfaces. Since a parallel manipulator becomes uncontrollable on a singular configuration, the possibility to change its assembly-mode without encountering a singularity is interesting as it can enlarge its usable workspace. Knowing whether a parallel manipulator has this feature is of interest for both the designer and the end-user. The second-order singularities, which form cusp points in plane sections of the joint space, play an important role in non-singular assembly-mode changing motions. Indeed, encircling a cusp point makes it possible to execute such motions [5], [9], [12]–[19]. A special class of planar 3-RPR manipulators has been studied recently [9], [10]. These manipulators have

the peculiarity that the resolution of the direct kinematics problem is split into a cubic equation and a quadratic equation. Their geometry is characterized by the fact that the platform triangle is congruent to the base triangle via an indirect isometry of the plane; this is the reason why we call them “symmetric”.

We propose here a coordinate system for the workspace which is adapted to this specific class and reflects the splitting of the direct kinematic problem (section II). We pay attention to the description of singularities (section III) and cusps (section IV) using these coordinates. We show how to sort assembly modes and use this sorting to do motion planning in the joint space (section V).

II. ALTERNATIVE COORDINATES FOR THE WORKSPACE

The base triangle is denoted by $A_1A_2A_3$. In the direct orthonormal frame \mathcal{F} with origin A_1 and first axis oriented by $\overrightarrow{A_1A_2}$, the coordinates of A_2 are $(b, 0)$ and those of A_3 are (d, h) . The platform triangle is denoted by $B_1B_2B_3$. Due to the symmetry property, the coordinates of B_2 and B_3 in the direct orthonormal frame with origin B_1 and first axis oriented by $\overrightarrow{B_1B_2}$ are respectively $(b, 0)$ and $(d, -h)$. The length of the leg A_iB_i is as usual denoted by ρ_i .

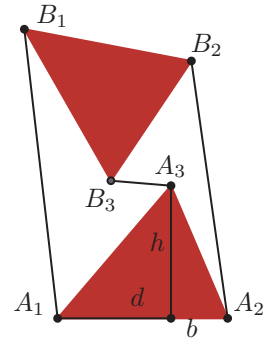


Fig. 1. A symmetric 3-RPR manipulator.

The platform triangle $B_1B_2B_3$ is the image of the base triangle $A_1A_2A_3$ by a glide reflection S . We encode this glide reflection S by the triple (ψ, r, g) such that the glide reflection is the orthogonal symmetry with respect to the line Δ with equation $x \cos(\psi) + y \sin(\psi) - r = 0$ followed by the translation of vector $2g \begin{pmatrix} -\sin(\psi) \\ \cos(\psi) \end{pmatrix}$ parallel to the symmetry axis (the equation of Δ and the coordinates of the translation vector are given in frame \mathcal{F} attached to the base triangle - see figure 2).

We choose the angle ψ in $[-\pi/2, \pi/2]$ and make the identification of $(-\pi/2, r, g)$ with $(\pi/2, -r, -g)$.

The research work reported here was made possible by SiRoPa ANR Project.

M. Coste is with Institut de Recherche Mathématique de Rennes, Université de Rennes I, Campus de Beaulieu, 35042 Rennes, France michel.coste@univ-rennes1.fr

P. Wenger and D. Chablat are with Institut de Recherche en Communications et Cybernétique de Nantes, 1 rue de la noë, 44321 Nantes, France Philippe.Wenger@irccyn.ec-nantes.fr, Damien.Chablat@irccyn.ec-nantes.fr

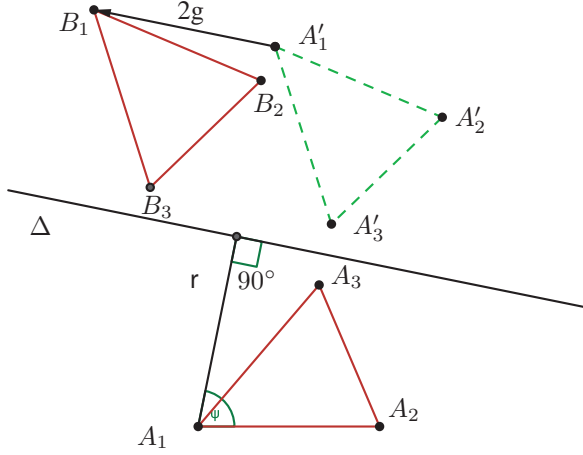


Fig. 2. The glide reflection sending $A_1A_2A_3$ to $B_1B_2B_3$.

Usually the workspace is viewed as the space of rigid motions in the plane and a pose of the manipulator is encoded by the rigid motion R carrying the half-line $[A_1A_2]$ to the half-line $[B_1B_2]$. The rigid motion R and the glide reflection S are related in the following way: S is the orthogonal symmetry with respect to (A_1A_2) followed by R . If the rigid motion R is given (as in [9], for instance) by the angle of rotation φ and the translation vector $\begin{pmatrix} x \\ y \end{pmatrix}$, then the relation between the two systems of coordinates is as follows:

$$\varphi = 2\psi + \pi \pmod{2\pi} \quad (1)$$

$$x = 2(r \cos(\psi) - g \sin(\psi)) \quad (2)$$

$$y = 2(r \sin(\psi) + g \cos(\psi)) . \quad (3)$$

It is easy to compute the lengths ρ_i of the legs A_iB_i in terms of (ψ, r, g) , since B_i is the image of A_i by the glide reflection. The square ρ_i^2 is the sum of the square of the double of the distance of A_i to the axis Δ and the square of the norm of the translation vector, which is $4g^2$. This gives:

$$\rho_1^2 = 4(r^2 + g^2) , \quad (4)$$

$$\rho_2^2 = 4((b \cos(\psi) - r)^2 + g^2) , \quad (5)$$

$$\rho_3^2 = 4((d \cos(\psi) + h \sin(\psi) - r)^2 + g^2) . \quad (6)$$

It will be convenient to introduce $\delta_2 = (\rho_2^2 - \rho_1^2)/4$ and $\delta_3 = (\rho_3^2 - \rho_1^2)/4$. These quantities depend only on ψ and r , and not on g :

$$\delta_2 = -2b \cos(\psi) r + b^2 (\cos(\psi))^2 , \quad (7)$$

$$\delta_3 = (d \cos(\psi) + h \sin(\psi))^2 - 2r(d \cos(\psi) + h \sin(\psi)) \quad (8)$$

Eliminating r between these two equations and writing the equation obtained in $t = \tan(\psi)$, we get the third degree equation:

$$\delta_2 h t^3 + (b h^2 - b \delta_3 + \delta_2 d) t^2 + (2 b d h - b^2 h + \delta_2 h) t - b \delta_3 + \delta_2 d + b d^2 - b^2 d = 0 . \quad (9)$$

This equation is essentially the same as the third degree characteristic polynomial obtained in [10].

We shall use $(\rho_1^2, \rho_2^2, \rho_3^2)$ as coordinates for the actuated joint space. Of course, this joint space is contained in the positive orthant $(\mathbb{R}_+)^3$.

The direct kinematic problem (DKP) can be solved as follows:

- 1) Take a real solution in t of equation (9), which determines $\psi = \arctan(t)$. Generically there are 3 or 1 real solutions, depending on the sign of the discriminant of the equation.
- 2) Compute r from ψ using equation (7), which gives

$$r = \frac{1}{2} \left(b \cos(\psi) - \frac{\delta_2}{b \cos(\psi)} \right) . \quad (10)$$

- 3) Solve the equation (4) for g . It has two real opposite solutions when $\rho_1^2 > 4r^2$.

One should take care in the resolution of the DKP of the case $\psi = \pm\pi/2$, i.e. $t = \infty$. This corresponds to the vanishing of the third degree term in equation (9), which occurs when $\delta_2 = 0$. In this case one can use equation (8) to compute r , which gives $r = (h^2 - \delta_3)/2h$ for $\psi = \pi/2$.

Note that the existence of a solution to the DKP depends

- first, on the existence of a solution (ψ, r) to the system of equations (7) and (8),
- second, given such a solution (ψ, r) , on the existence of a solution g to equation (4).

These two conditions of existence will be important for the discussion of singularities in the next section.

III. SINGULARITIES

The singular surface in the actuated joint space is thus given as the union of two surfaces S_1 and S_2 , corresponding respectively to steps 1 and 3 of the resolution of the DKP described above. The fact that the singular surface splits in two components has already been observed in [9]. We will now describe these two surfaces. We will also describe the critical surfaces Σ_1 and Σ_2 in the workspace, whose images by the mapping $(\psi, r, g) \mapsto (\rho_1^2, \rho_2^2, \rho_3^2)$ given by equations (4), (5) and (6) are S_1 and S_2 respectively.

A. The first singular surface

The surface S_1 is the intersection of the actuated joint space (always with coordinates $(\rho_1^2, \rho_2^2, \rho_3^2)$) with a cylinder having generatrix parallel to $(1, 1, 1)$ and basis a curve C in the plane of coordinates (δ_2, δ_3) . An equation for C can be obtained as the discriminant of equation (9); it is a quartic. An alternative way to describe C is to compute the jacobian determinant of the mapping $\Phi : (\psi, r) \mapsto (\delta_2, \delta_3)$ given by equations (7) and (8). The jacobian curve Γ in the space with coordinates (ψ, r) is given by

$$r = \frac{\cos(\psi)}{h} \left(\frac{(h^2 + b d - d^2) \cos(\psi) \sin(\psi) +}{(2d - b) h \cos(\psi)^2 + (b - d) h} \right) . \quad (11)$$

Observe that $r(\psi + \pi) = -r(\psi)$. The critical surface Σ_1 in the workspace is the set of all (ψ, r, g) such that (ψ, r) belongs to Γ . The curve C is the image of Γ by the mapping

Φ , and it can be parameterized by rational functions of $t = \tan(\psi)$ as

$$\begin{cases} \delta_2 = \frac{b((2d-b)ht^2 + (2d^2 - 2bd - 2h^2)t + (b-2d)h)}{(1+t^2)^2 h} \\ \delta_3 = \frac{(ht+d)^2(ht^2 + 2(d-b)t - h)}{(1+t^2)^2 h} \end{cases} \quad (12)$$

So C is indeed a rational quartic. Its singular points are three real cusps that can be found by looking at the stationary points of the parameterization. These stationary points correspond to parameters t which are roots of the cubic equation

$$(b-2d)ht^3 + 3(h^2-d^2+db)t^2 + 3h(2d-b)t + d^2-dh-h^2 = 0. \quad (13)$$

Since the discriminant $108(d^2+h^2)^2((d-b)^2+h^2)^2$ of this cubic equation is strictly positive, there are always three real roots and hence three real cusps on the curve C . Actually, transforming the equation to an equation in ψ , one obtains

$$\tan(3\psi) = \frac{d^2 - bd - h^2}{(b-2d)h} \quad (14)$$

Note that the curve C has no other singular point than the three cusps. Indeed, a rational quartic may have only up to three singular points. The curve C always has the shape of a deltoid, i.e. a closed curve with three cusps connected by arcs concave to the exterior.

B. The second singular surface

The second critical surface Σ_2 in the workspace is simply given by $g = 0$; so it is independent of the geometry of the manipulator (this is already observed in [9]). Its image S_2 in the actuated joint space is parameterized by substituting $g = 0$ in equations (4-6). So the surface S_2 is the image of the elliptic cylinder

$$\rho_1 = 2r, \quad (15)$$

$$\rho_2 = 2(r - b \cos(\psi)), \quad (16)$$

$$\rho_3 = 2(r - d \cos(\psi) - h \sin(\psi)) \quad (17)$$

by the mapping $(\rho_1, \rho_2, \rho_3) \mapsto (\rho_1^2, \rho_2^2, \rho_3^2)$. The implicit equation of S_2 can also be obtained by eliminating t between equation (9) and the equation

$$\rho_1^2 = \frac{\delta_2^2(1+t^2)}{b^2} - 2\delta_2 + \frac{b^2}{1+t^2},$$

where the right hand side is the expression for $4r^2$ derived from (10). The implicit equation for S_2 obtained in this way is a quartic equation in $\rho_1^2, \rho_2^2, \rho_3^2$, not a very nice one.

C. An example

We consider the manipulator with parameters $b = 1, h = 1, d = 0$. In this case the curve C in the plane (δ_2, δ_3) is a hypocycloid with three cusps (a deltoid) inscribed in the circle with center $(1/4, 1/4)$ and radius $\sqrt{9/8}$. The three cusps on C correspond to the values $-\frac{5\pi}{12}, -\frac{\pi}{12}, \frac{\pi}{4}$ of ψ .

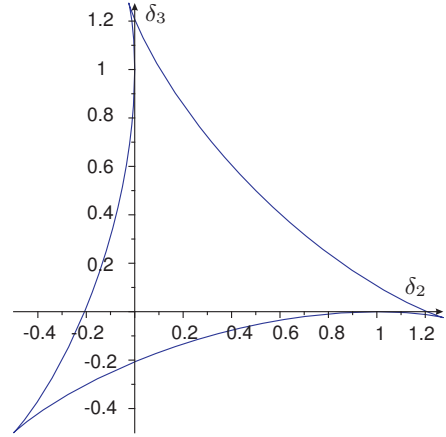


Fig. 3. The curve C

The critical surface Σ_2 in the workspace is always given by $g = 0$. The critical surface Σ_1 is parameterized by

$$(\psi, -\cos(\psi)(-1 - \sin(\psi)\cos(\psi) + \cos(\psi)^2), g).$$

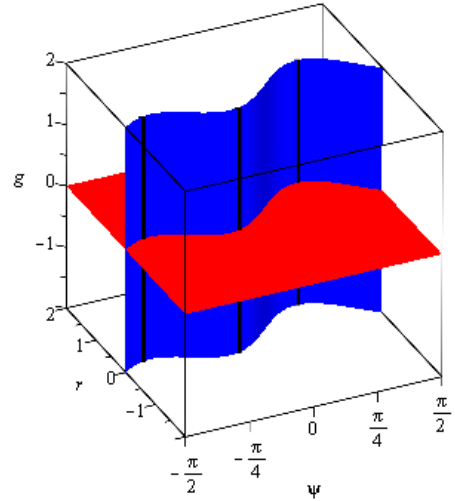


Fig. 4. The critical surfaces Σ_1 (in blue) and Σ_2 (in red).

Both critical surfaces are represented in figure 4. It may be interesting to compare this figure with figure 2 in [9], which represents the same surfaces (with the same color code), but in a different coordinate system. The choice of coordinates made here “straightens” the critical surfaces.

The three black lines of figure 4 are the lines of points which correspond to cusps in the joint space.

We represent now the singular surfaces S_1 and S_2 in the joint space (See figures 5 and 6). The surface S_1 is a part of a cylinder on the hypocycloid and has three half-lines of cusps. The drawing of the singular surfaces is made using their parameterizations by (ψ, g) for S_1 and by (ψ, r) for S_2 .

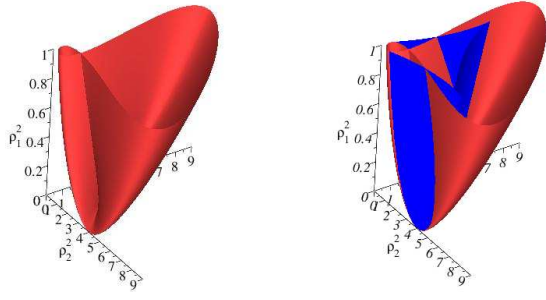


Fig. 5. S_1 (in blue) and S_2 (in red) cut at $\rho_1^2 = 1$.

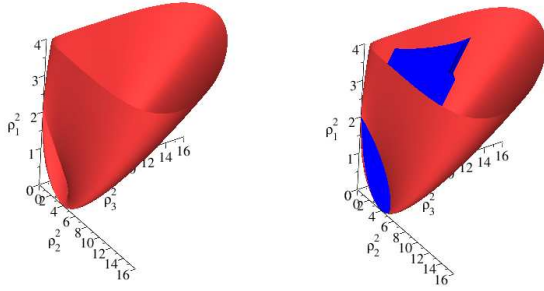


Fig. 6. S_1 (in blue) and S_2 (in red) cut at $\rho_1^2 = 4$.

IV. CUSPS

The singular surface S_1 has three half-lines of cusps, all parallel to the vector $(1, 1, 1)$. So the cusps are entirely determined once we know the origins of these three half-lines. The three possible angles ψ are determined by equation (14):

$$\psi_{\text{cusp}} = \frac{1}{3} \arctan\left(\frac{d^2 - bd - h^2}{(b - 2d)h}\right) + k \frac{\pi}{3} \pmod{\pi}$$

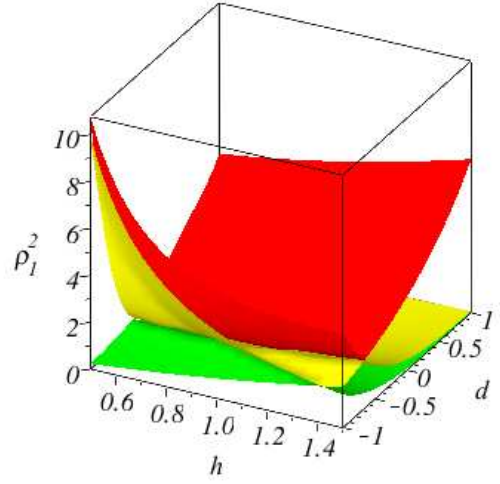
for $k = 0, 1, 2$. For each of these three values of ψ_{cusp} , the corresponding value r_{cusp} is given by equation (11). The couple $(\psi_{\text{cusp}}, r_{\text{cusp}})$ determines the line supporting the half-line of cusps, and the origin of this half-line corresponds to $g = 0$. So we get three values for the ρ_1^2 of the origins of the three half-lines of cusps, which are the three values for $4r_{\text{cusp}}^2$. These three values for ρ_1^2 are the roots of a third degree polynomial with coefficients depending on b, h, d ; the constant term of this polynomial is

$$4h^2(-2d+b)^2(d^3-2bd^2+h^2d+b^2d-2bh^2)^2(-h^2+2bd-d^2)^2,$$

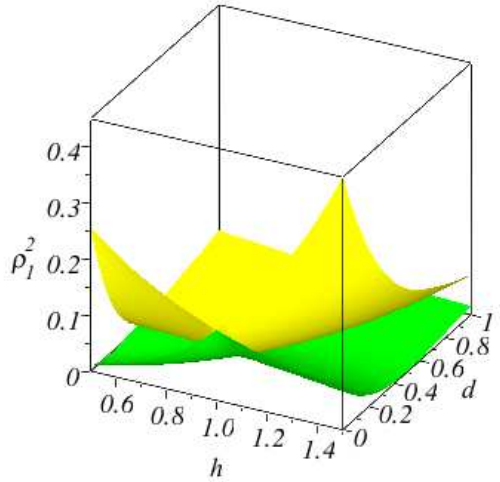
and its discriminant is always nonnegative.

Let $0 \leq \beta_1 \leq \beta_2 \leq \beta_3$ be the three bifurcation values of ρ_1^2 for the number of cusps, i.e. the ρ_1^2 of the origins of the half-lines of cusps. Then the slice at $\rho_1^2 = c$ has 0 cusp if $0 \leq c < \beta_1$, 1 if $\beta_1 < c < \beta_2$, 2 if $\beta_2 < c < \beta_3$ and 3 if $\beta_3 < c$. One of the bounded intervals may be empty, if the constant term of the equation of the third degree in ρ_1^2 vanishes (for the first interval) or if its discriminant vanishes (for the second or third interval). One has to understand that

the number of cusps is the number of cusp points in the slice of the joint space. Over each of these cusps there are two triple solutions of the DKP, corresponding to opposite values of g .



(a)



(b)

Fig. 7. The bifurcation values of ρ_1^2 for the number of cusps.

Figure 7a represents the bifurcation values as function of h and d , with b fixed equal to 1 (green for β_1 , yellow for β_2 and red for β_3). Figure 7b shows detail for the first and second bifurcation values when $0 \leq d \leq 1$.

V. SORTING ASSEMBLY MODES AND MOTION PLANNING IN THE JOINT SPACE

The essential idea here is the following: when one starts from a nonsingular solution of the DKP at a point in the

joint space with coordinates $(\rho_1^2, \rho_2^2, \rho_3^2)$ and moves in the direction of the vector $(1, 1, 1)$, then the solution of the DKP follows smoothly, without crossing a singularity in the workspace. Indeed, consider equations (4-6): the motion $\rho_i^2 \mapsto \rho_i^2 + \lambda^2$, increasing λ , can be lifted in the workspace (with coordinates (ψ, r, g)) to a path with ψ and r fixed and g increasing to $g^2 + \lambda^2/4$.

The segment in the joint space can cross the second singular surface S_2 . This corresponds to the appearance of two new solutions to the DKP (one in each aspect), with a different couple (ψ, r) . But it never crosses the first singular surface S_1 which is a cylinder with generatrix parallel to $(1, 1, 1)$.

We denote $\rho_1^2 + \rho_2^2 + \rho_3^2$ by ν . Then $(\nu, \delta_2, \delta_3)$ form a system of coordinates for the joint space which is convenient for our present discussion. Moving in the joint space in the direction of the vector $(1, 1, 1)$ is increasing ν , keeping δ_2 and δ_3 fixed.

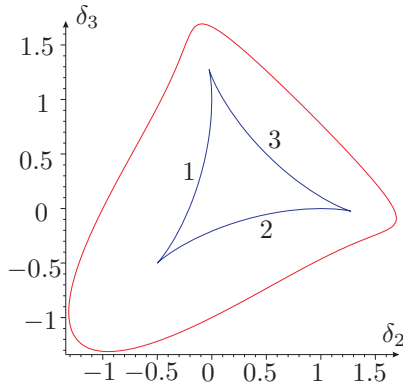


Fig. 8. The section $\nu = 8$.

The situation in the section $\nu = k$ stabilizes for sufficiently large values of k : the section of S_2 is a big oval surrounding the section of S_1 which is a deltoid with three cusps (the curve C , base of the cylinder). Inside this curve C there are, in each aspect, three continuous solutions of the DKP and between this curve C and the section of S_2 there is in the same aspect one continuous solution of the DKP. Label by 0 this solution, and label by 1, 2, 3 the three arcs of C between the cusps. Then we can label the three solutions inside the deltoid C by 1, 2, 3 according to the label of the arc of the deltoid through which they are connected with the solution 0. Figure 8 illustrates the labelling in the same example as above (the coordinates (δ_2, δ_3) are used in the section $\nu = 8$).

In this way we can label every solution of the DKP contained in one aspect by one of the labels 0, 1, 2 or 3. In each aspect, all points in the same label form a connected region and the boundaries between these regions are the so-called “characteristic surfaces” obtained by pulling back the singular surface S_1 in the aspect [20]. The characteristic surfaces in the workspace with coordinates (ψ, r, g) are cylinders with generatrix parallel to the g -axis and basis the

two curves in the (ψ, r) plane which are given by

$$r = \frac{h(2d+b)\cos(\psi) + (h^2 + bd - d^2)\sin(\psi)}{4h} \pm \frac{\sqrt{(h^2 + d^2)(h^2 + d^2 + b^2 - 2bd)}}{4h}$$

Figure 9 represents a section of the characteristic surfaces (in green) by a plane $g = \text{constant}$ of the workspace. The blue curve is a section of Σ_1 and separates the aspects. In each aspect, the characteristic surface delimitates the four sorts of assembly modes. The label 0 correspond to points which are mapped outside of the deltoid C in the joint space, and the labels 1, 2, 3 to points which are mapped inside. A path from 0 to 1 inside an aspect is mapped to a path going through the arc of the deltoid with label 1, etc..

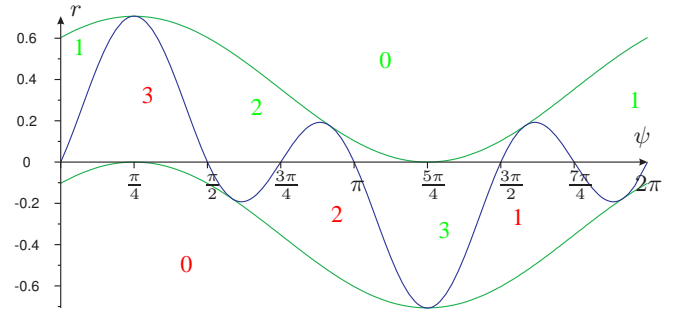


Fig. 9. The four sorts of assembly modes in each aspect, in a section $g = \text{constant}$ of the workspace. The green curves are sections of the characteristic surfaces.

We illustrate how the labelling can be used for motion planning in the joint space with an example, again for the manipulator with parameters $b = 1, h = 1, d = 0$. We choose a goal position for the manipulator, given by $\psi = \pi/4, r = 1.1$ and $g = 0.4$ (Figure 10).

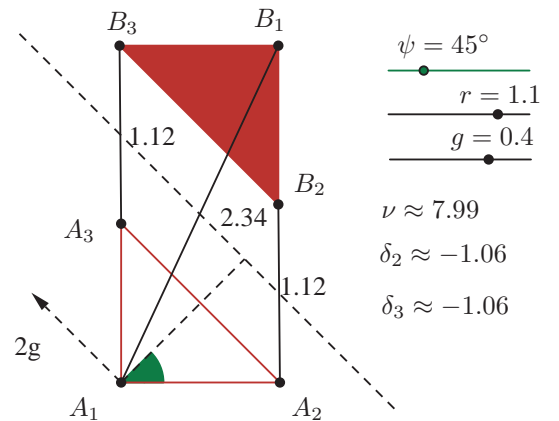


Fig. 10. The goal position.

The goal position corresponds to values $\rho_1 \approx 2.34, \rho_2 = \rho_3 \approx 1.12$ and $\nu \approx 7.99$; it is labelled 0 and mapped outside of the deltoid in the joint space. We explain how to plan (in the joint space) a path to the goal position

from a position of the manipulator in the same aspect, with $\nu \leq 7.99$. The starting position corresponds to $\rho_1^0, \rho_2^0, \rho_3^0$ and label $\ell \in \{0, 1, 2, 3\}$.

- Increase simultaneously ρ_1, ρ_2, ρ_3 following $\rho_i = \sqrt{(\rho_i^0)^2 + t^2}$ until $\nu = \sum \rho_i^2 = 8$
- Keeping $\nu = 8$ constant, move in the plane with coordinates (δ_2, δ_3) from

$$(\delta_2^0 = (\rho_2^0)^2 - (\rho_1^0)^2, \delta_3^0 = (\rho_3^0)^2 - (\rho_1^0)^2)$$

to $(-1.06, -1.06)$ following a path inside the red curve and crossing only arc $\# \ell$ of the deltoid if the label is ℓ .

Figure 11 shows such a path for label $\ell = 3$. (Actually, it shows only the part of the path in the plane (δ_2, δ_3) for $\nu = 8$, since the first segment of the path increases ν without changing δ_2 nor δ_3).

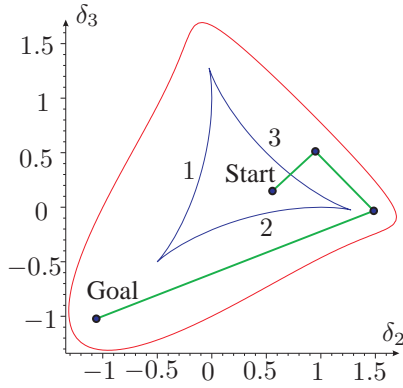


Fig. 11. A path from a starting and a goal position

VI. CONCLUSIONS

The choice of coordinates for the workspace well adapted to the special class of symmetric manipulators allowed us to take full advantage of the de-coupling of DKP (into a cubic and a quadratic equation) in the computations. We obtained rational parameterizations of the singular surfaces in the joint space. We obtained also a good description of the cusp curves on these surfaces, as well as precise information on the bifurcation of the number of cusps in the slices of the joint space. Finally, we were able to sort assembly modes in an aspect and to use this sorting for motion planning in the joint space.

REFERENCES

- [1] K. H. Hunt, "Structural Kinematics of In Parallel-Actuated Robot-Arms," *Journal of Mechanisms, Transmissions and Automation in Design*, Vol. 105, pp. 705-712, December 1983.
- [2] K. H. Hunt, E. J. F. Primrose, "Assembly Configurations of some In-Parallel-Actuated Manipulators," *Mechanism and Machine Theory*, Vol. 28, N° 1, pp. 31-42, 1993.
- [3] N. Rojas, F. Thomas, "The Forward Kinematics of 3-RPR Planar Robots: A Review and a Distance-Based Formulation," *IEEE Transactions on Robotics*, Vol. 27 (1), February 2011.
- [4] C. Innocenti, V. Parenti-Castelli, "Singularity-free evolution from one configuration to another in serial and fully-parallel manipulators," *ASME Robot, Spatial Mechanisms and Mechanical Systems*, vol. 45, pp. 553-560, 1992.

- [5] P.R. Mcaree, R.W. Daniel, "An explanation of never-special assembly changing motions for 3-3 parallel manipulators," *The International Journal of Robotics Research* 18 (6) (1999) 556-574.
- [6] X. Kong, C.M. Gosselin, "Forward displacement analysis of third-class analytic 3-RPR planar parallel manipulators," *Mechanism and Machine Theory*, 36:1009-1018, 2001.
- [7] L. Husty M., "Non-singular assembly mode change in 3-RPR-parallel manipulators," In *Proceedings of the 5th International Workshop on computational Kinematics*, pp. 43-50, Kecskeméthy, A., Müller, A. (eds.), 16 April 2009.
- [8] P. Wenger, D. Chablat, "Workspace and Assembly modes in Fully-Parallel Manipulators: A Descriptive Study," *Advances in Robot Kinematics: Analysis and Control*, Kluwer Academic Publishers, pp. 117-126, 1998.
- [9] P. Wenger, D. Chablat, "Kinematic analysis of a class of analytic planar 3-RPR parallel manipulators," *Proceedings of CK2009, International Workshop on Computational Kinematics*, Duisburg, May 5-8, 2009.
- [10] P. Wenger, D. Chablat et M. Zein, "Degeneracy study of the forward kinematics of planar 3-RPR parallel manipulators," *ASME Journal of Mechanical Design*, Vol 129(12), pp 1265-1268, 2007.
- [11] M. Zein, P. Wenger, D. Chablat, "Singular curves and cusp points in the joint space of 3-RPR parallel manipulators," in: *Proceedings of IEEE International Conference on Robotics and Automation*, Orlando, May 2006.
- [12] M. Zein, P. Wenger, D. Chablat, "Non-singular assembly-mode changing motions for 3-RPR parallel manipulators," *Mechanism and Machine Theory* 43(4), 480-490, Jun 2007.
- [13] E. Macho, O. Altuzarra, C. Pinto, and A. Hernandez, "Singularity free change of assembly mode in parallel manipulators: Application to the 3RPR planar platform," presented at the 12th IFToMM World Congr., Besancon, France, Jun. 18-21, 2007, Paper 801.
- [14] H. Bamberger, A. Wolf, and M. Shoham, "Assembly mode changing in parallel Mechanisms," *IEEE Transactions on Robotics*, 24(4), pp. 765-772, 2008.
- [15] E. Macho, E. Altuzarra, O., Pinto, C., and Hernandez, A., "Transitions between multiple solutions of the Direct Kinematic Problem," 11th International Symposium Advances in Robot Kinematics, June 22-26, 2008, France.
- [16] A. Hernandez, O. Altuzarra, V. Petuya, and E. Macho., "Defining conditions for non singular transitions of assembly mode," *IEEE Transactions on robotics*, 25(6):1438-1447, 2008.
- [17] M. Urizar, V. Petuya, O. Altuzarra and A. Hernandez, "Computing the Configuration Space for Motion Planning between Assembly Modes," *Computational Kinematics Proceedings of the 5th International Workshop on Computational Kinematics*, Thursday 6 October 2009.
- [18] M. Urizar, V. Petuya, O. Altuzarra, E. Macho and A. Hernandez, "Analysis of the Direct Kinematic Problem in 3-DOF Parallel Manipulators," *SYROM 2009 Proceedings of the 10th IFToMM International Symposium on Science of Mechanisms and Machines*, held in Brasov, Romania, October 12-15, 2009.
- [19] M. Urizar, V. Petuya, O. Altuzarra and A. Hernandez, "Researching into nonsingular transitions in the joint space," *Advances in Robot Kinematics: Motion in Man and Machine*, Piran Portoroz, Slovenia, Springer 45-52, Monday, June 28, 2010.
- [20] P. Wenger, D. Chablat, "Definition Sets for the Direct Kinematics of Parallel Manipulators," *International Conference Advanced Robotics*, pp. 859-864, 1997.